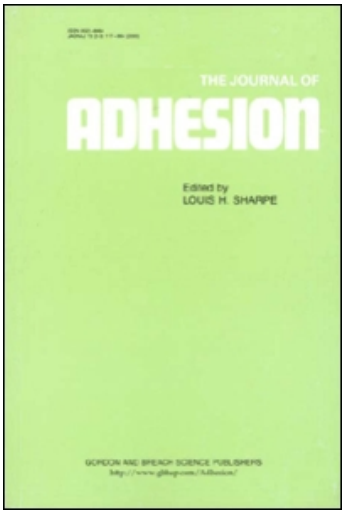

The Journal of Adhesion
Publication details, including instructions for authors and subscription information:
http://www.informaworld.com/smpp/title~content=t713453635

Non-linear Modeling of Tubular Adhesive Scarf Joints Loaded in Tension

Vu Nguyen[a]; Keith T. Kedward[a]
[a] Department of Mechanical and Environmental Engineering, University of California, Santa Barbara, CA, USA

To cite this Article Nguyen, Vu and Kedward, Keith T.(2001) 'Non-linear Modeling of Tubular Adhesive Scarf Joints Loaded in Tension', The Journal of Adhesion, 76: 3, 265 — 292
To link to this Article: DOI: 10.1080/00218460108029629
URL: http://dx.doi.org/10.1080/00218460108029629

J. Adhesion, 2001, Vol. 76, pp. 265–292
Reprints available directly from the publisher
Photocopying permitted by license only

Non-linear Modeling of Tubular Adhesive Scarf Joints Loaded in Tension

VU NGUYEN* and KEITH T. KEDWARD†

Department of Mechanical and Environmental Engineering, University of California, Santa Barbara, CA 93106, USA

(Received 10 November 2000; In final form 8 March 2001)

In this paper, a simple analytical model is developed to determine the adhesive shear strain distribution of a tubular adhesive scarf joint loaded in tension. The approach is an extension of the original well-recognized Volkersen's shear lag analysis for a shear loaded joint, which is frequently applied to adhesively-bonded joints. A mathematical representation consisting of linear and exponential functions is employed to model the elastic–plastic behavior commonly observed in structural adhesives. The governing equation is found to be in the form of a non-linear second-degree ordinary differential equation with variable coefficients. A numerical method required for solving this equation is also introduced. Numerical predictions of shear strain distributions are compared with results from non-linear Finite Element Analysis (FEA), utilizing the commercially available software, ANSYS 5.6, a general-purpose software system. It is shown that both the linear and non-linear approximate solutions are closely comparable with the FEA results for a 10°-scarf angle and elastic isotropic adherends. In concurrence with previous work on flat adherends, the present work demonstrates that the scarf joint develops more uniform shear stress and strain distributions with a consequent reduction in peak values than those for the conventional lap joint. In contrast, the conventional lap joint with the equivalent bonded surface area experiences a more substantial elastic trough, which can provide a more stable configuration for, sustained long term loading applications.

Keywords: Tubular adhesive scarf joint; Volkersen's shear lag theory; Non-linear shear behavior; Linear-exponential representation; Non-linear FEA

*Address for correspondence: Indigo Systems Corporation, 5385 Hollister Avenue, Santa Barbara, CA 93111, USA.
†Corresponding author. Tel.: 805-893-3381, Fax: 804-893-8651, e-mail: kedward@engineering.ucsb.edu

INTRODUCTION

Adhesive bonding has increasingly been selected as an attractive method for joining critical mechanical components and structures. It exhibits many advantages such as lighter weight, more uniform stress distributions, smoother load transfer and, potentially, longer fatigue life over other traditional joining methods. In joining tubular components, adhesive bonding is even more appealing, since it eliminates complex machined features that are necessarily prepared for mechanical fasteners. For the last four decades, numerous adhesive bonding projects have been conducted in both theoretical and experimental fields. However, significantly less effort has been expended in adhesive bonding researches of tubular joints, with or without considering the non-linearity of an adhesive, relative to that of flat lap joints. Figure 1 depicts a simple representation of the tubular scarf joint with, its geometrical joint parameters, that is investigated in this study.

The first analytical treatment of a general adhesive scarf joint was proposed by Lubkin [1] for an ideally sharp, flat scarf joint loaded in tension with assumptions of zero bending moments and a uniform state of stress and based on linear adhesive characteristics. Lubkin pointed out that no stress concentrations were found at the

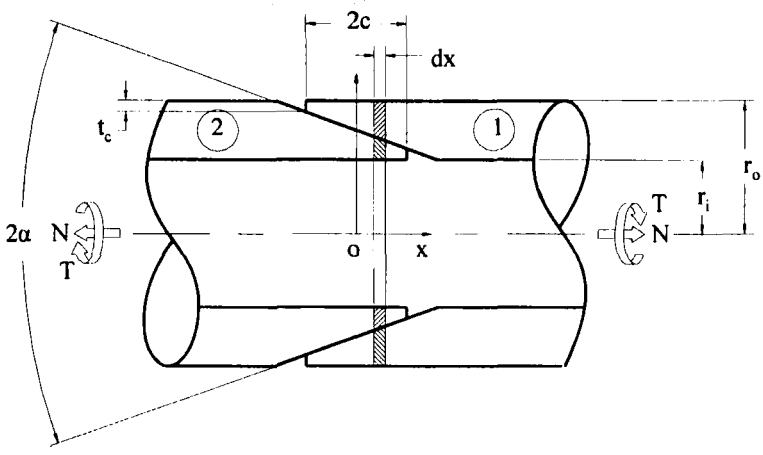

FIGURE 1 Scarf joint geometry, joint parameters, and loading configurations.

two joint terminations and that the theory was valid at any angle if similar-material adherends were used. For dissimilar materials, it was also claimed that there existed an angle in which Lubkin's theory would hold. Adams and Peppiatt [2] employed Finite Element Analysis (FEA) utilizing 8-node iso-parametric elements and linear elasticity to analyze a tubular scarf joint, referenced as a tapered joint, in both tension and torsion. In 1990, Chen and Cheng [3] tried to resolve Thein's [4] plane stress scarf joint problem using linear elasticity theory and the variational principles of complementary energy. New criteria were introduced to replace Lubkin's criteria for uniform stress state. Periodically, between 1973 and 1981, Hart-Smith [5,6] proposed and refined an entirely different approach to investigate analytically a flat scarf joint in tension. He developed a method to compute the shear stress distributions in the adhesive of a multiple-step flat lap joint. The method is based on the shear lag theory that had been introduced by Volkersen [7] for shear stress calculations of a single flat lap joint. By increasing the number of steps to infinity, the scarf joint solution, in theory, could eventually be obtained by iterative techniques.

Most studies have assumed a linear elastic behavior for structural adhesives while most adhesives, either ductile or brittle, exhibit some form of non-linearity especially when subjected to shear loads. Some treatments of adhesive non-linearity, however, have been proposed over the years. Hart-Smith [6,8] extended a linear-elastic-perfectly-plastic model. The Engineering Services Data Units (ESDU) in the United Kingdom [9] and Hughes Aircraft Company [10] employed a piecewise-linear approximation. Nagaraja and Alwar [11] used non-linear FEA, and Adams and Mallick [12] introduced the Effective Modulus Method. Hart-Smith, ESDU and Hughes Aircraft have modeled a non-linear adhesive as an elastic–plastic material with different idealizations of shear stress–strain behaviors. These properties are typically measured using a thick adherend coupon according to ASTM-D-5656 in conjunction with test with a KGR extensometer [13–16] or a pure shear test of a cast-and-machined cylindrical "hour-glass" shaped specimen [17]. Conversely, non-linear FEA method and Effective Modulus Method require information from the uniaxial stress–strain relationship that is usually obtained by testing the molded bulk form of an adhesive in tension,

ASTM-D-638, or in compression, ASTM-D-695. When being tested in a uniaxial tension test, an adhesive is significantly more sensitive to defects and voids than in a shear test, which reflects real service conditions. Therefore, it is believed that as an adhesive is primarily loaded in shear except at the terminations, the shear data are more appropriate for supporting shear strain calculations and for strength predictions than the uniaxial data. If required for FEA, an equivalent uniaxial stress–strain relationship based on the adhesive shear behavior and Von-Mises's combined-stress criteria should be established and employed.

Today, Finite Element Analysis (FEA), as a widely-used, numerically approximate method, has become a very powerful tool for the study of adhesive joints. However, FEA can be quite expensive in terms of time and labor to set up and to execute since it usually requires a new computer run for each change in value of any parameters involved for a parametric study. It is even significantly more time-consuming when adhesive non-linearity is involved. Therefore, a simple numerical method based on an analytical treatment can be found useful and quite efficient in this problem for design and analysis purposes. One-dimensional modeling and analysis of a tubular scarf joint loaded in tension are performed and presented. In addition, a non-linear representation of an adhesive will also be proposed and introduced into the joint modeling. Nevertheless, FEA is still considered as a highly acceptable tool for the verification of an analytical study or for problems that preclude the application of analytical solutions. Moreover, the method has become a standard for mechanical engineering analyses and for verification of approximate analytical solutions. Thus, in this paper non-linear Finite Element Analyses is employed to access the developed theory.

DERIVATION OF GOVERNING EQUATION

It is assumed that the non-linear characteristic of an adhesive illustrated in Figure 2 has the stress-explicit form of a combination of linear and exponential functions as follows:

$$\tau = B_0\gamma + B_1(1 - e^{-k\gamma}) \tag{1}$$

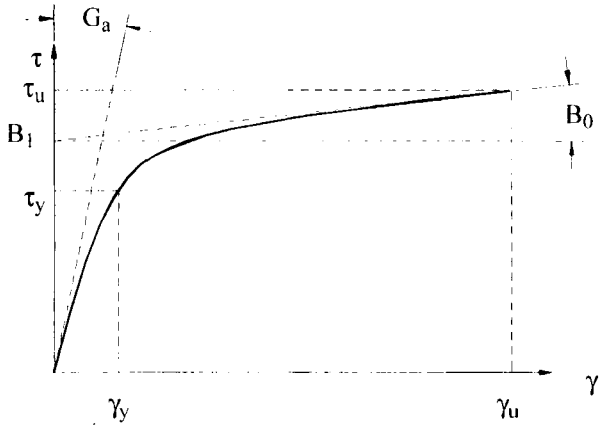

FIGURE 2 Proposed linear and exponential idealization of an adhesive loaded in shear.

then the initial shear modulus, G_a, that is the initial gradient of the function at $\gamma = 0$, is related to two functional coefficients, B_0 and B_1, in Eq. (1) as

$$G_a = \left(\frac{d\tau}{d\gamma}\right)_{\gamma=0} = B_0 + kB_1 \tag{2}$$

Three fitting parameters are required to represent and fully define a specific adhesive system. In a special case observed for many ductile adhesives, *i.e.*, when B_0 approaches 0, the above function just can be simply reduced to

$$\tau = \tau_u\left(1 - e^{-(G_a/\tau_u)\gamma}\right) \tag{3}$$

where $B_1 =$ can be seen as the ultimate stress of the adhesive as illustrated in Figure 3. On the other hand, as B_1 approaches 0, the adhesive becomes linear elastic represented with the usual linear shear stress–strain relationship

$$\tau = G_a\gamma \tag{4}$$

Figure 4 depicts infinitesimal elements of a scarf joint in tension. The figure is grossly exaggerated for clarity. Assumptions made in

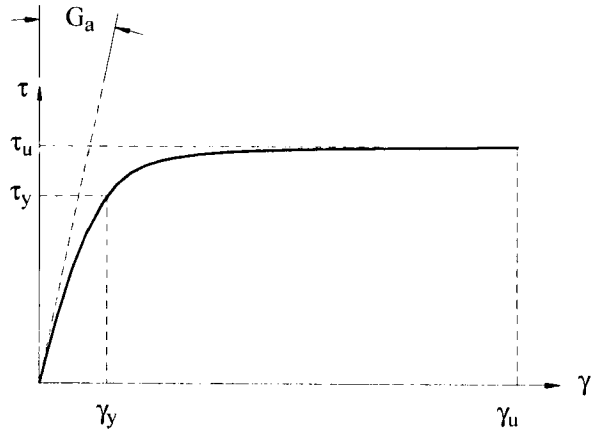

FIGURE 3 Proposed linear and exponential idealization of an adhesive loaded in shear.

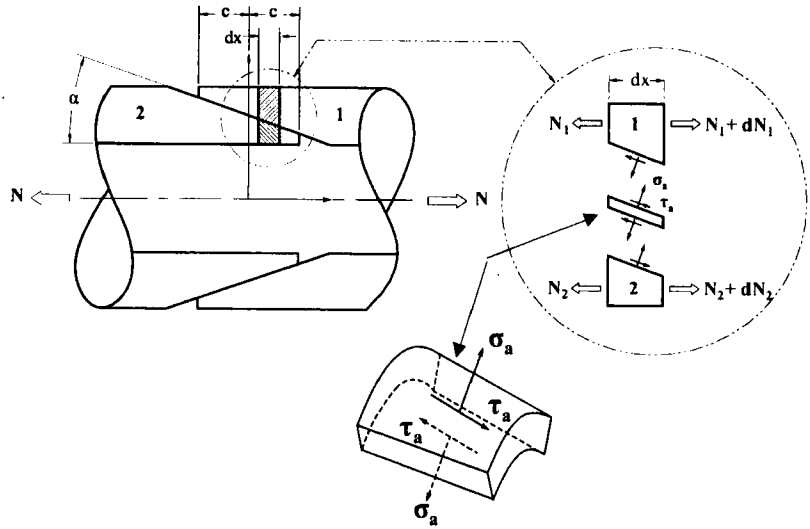

FIGURE 4 Infinitesimal elements in tension.

the derivations are:

(1) Adhesive is homogeneously isotropic and its behavior is described by Eq. (1).
(2) Adhesive is relatively thin and flexible.

(3) Uniform distribution of shear strain across the adhesive thickness.
(4) Adherends are homogeneously isotropic and linearly elastic.
(5) Hoop stress and deformation of the tubular adherends have negligible influence on the adhesive response.
(6) Neither axial tensile stresses nor axisymmetric bending is developed in the adhesive, based on the rather low adhesive modulus relative to the adherend modulii.
(7) Shear lag theory and differential strains are extended to include adhesive nonlinearity. This means only longitudinal tensile deformations in the tapered adherends and shear deformations in the adhesive layers are considered.

Consider the equilibrium condition of adherend 1; the following expressions can be obtained

$$-N_1 + N_1 + dN_1 - \tau_a 2\pi r dx \cos\alpha - \sigma_a 2\pi r dx \sin\alpha \approx 0 \tag{5}$$

$$-\tau_a 2\pi r ds \sin\alpha - \sigma_a 2\pi r dx \cos\alpha \approx 0 \tag{6}$$

or

$$\frac{dN_1}{dx}\frac{1}{2\pi r} \approx \tau_a \cos\alpha + \sigma_a \sin\alpha \tag{7}$$

$$\tau_a \sin\alpha \approx \sigma_a \cos\alpha \tag{8}$$

Adhesive shear deformation is approximated as

$$\gamma_a = \frac{1}{\tau_a}(u_1 - u_2)\cos\alpha \tag{9}$$

Since adhesive thickness is assumed sufficiently thin and flexible that it carries negligible axial load, at any cross section, equilibrium considerations yield the following relationship:

$$N = N_1 + N_2 \tag{10}$$

Differentiation of Eq. (9) with respect to x gives

$$\frac{d\gamma_a}{dx}\frac{t_a}{\cos\alpha} = \varepsilon_1 - \varepsilon_2 = \frac{N_1}{A_1 E_1} - \frac{N_2}{A_2 E_2} \tag{11}$$

Further differentiation of Eq. (11) in conjunction with Eq. (10) leads to the expression

$$\frac{d^2\gamma_a}{dx^2}\frac{t_a}{\cos\alpha} = \frac{dN_1}{dx}\eta + N_1\mu + \frac{N}{A_2^2E_2}\frac{dA_2}{dx} \tag{12}$$

where

$$r = r_m - x\tan\alpha$$
$$A_1 = \pi(r_0^2 - r^2) \quad \text{and} \quad A_2 = \pi(r^2 - r_i^2)$$
$$\eta = \frac{1}{A_1E_1} + \frac{1}{A_2E_2} \quad \text{and} \quad \mu = \frac{d\eta}{dx}$$

Substitution of Eqs. (7) and (11) into Eq. (12) leads to the governing equation in the form of a second-degree ordinary differential equation (ODE)

$$\frac{d^2\gamma_a}{dx^2} = \frac{\mu}{\eta}\frac{d\gamma_a}{dx} + \frac{2\pi r\eta\cos\alpha}{t_a}(\tau_a\cos\alpha + \sigma_a\sin\alpha) + \left(\frac{\mu}{\eta} + \frac{1}{A_2}\frac{dA_2}{dx}\right)\frac{N\cos\alpha}{t_aA_2E_2} \tag{13}$$

Boundary conditions for this ODE are

$$x = -c \quad N_1 = 0$$
$$x = c \quad N_1 = N$$

Substitution of the above boundary conditions into (11) yields Neumann boundary conditions, which are given in terms of derivatives at boundaries

$$\left(\frac{d\gamma_a}{dx}\right)_{x=-c} = -\frac{\cos\alpha}{t_a}\frac{N}{A_{2(x=-c)}E_2} \tag{14}$$

$$\left(\frac{d\gamma_a}{dx}\right)_{x=c} = \frac{\cos\alpha}{t_a}\frac{N}{A_{1(x=c)}E_1} \tag{15}$$

It should be noted that both τ_a and σ_a in the ODE Eq. (13) are functions of x. Introducing the non-linear adhesive Eqs. (1) and (8)

into Eq. (13) appropriately, the following expression is attained:

$$\frac{d^2\gamma_a}{dx^2} = \frac{\mu}{\eta}\frac{d\gamma_a}{dx} + \frac{2\pi r\eta B_0}{t_a}\gamma_a + \frac{2\pi r\eta B_1}{t_a}(1 - e^{-k\gamma_a}) + \left(\frac{\mu}{\eta} + \frac{1}{A_2}\frac{dA_2}{dx}\right)\frac{N\cos\alpha}{t_a A_2 E_2} \tag{16}$$

There are some unique characteristics associated with the derivation process and the governing equation itself that are highlighted below:

(1) The formulation is developed based on strain variables rather than stress variables and all stress parameters are retained until the shear stress–strain relationship is introduced. An explicit expression of the shear stresses was the motivation for this original approach that circumvents unnecessary manipulation of stress functions and permits representation of the non-linear function for the adhesive layer. The proposed idealization of the adhesive shear stress–strain relationship appears to work really well with the derivation scheme.

(2) It is readily observed that the adhesive thickness has not been included in calculations of A_1 and A_2, since it is assumed to be relatively thin compared with the adherend sizes. The assumption is believed to have an insignificant effect on the values of A_1 and A_2. However, if required, the thickness can be easily incorporated.

(3) The governing equation is found to be a boundary value problem, expressed in the form of a second-degree non-linear differential equation, with variable coefficients and derivative boundary conditions. Numerical methods are typically required since the solution of this particular type of equation is generally more complex and it is not directly solvable. However, with a few modifications to existing methods, such as Runge-Kutta or Finite Difference, the solution is certainly attainable.

(4) Two boundary conditions can be expressed mathematically in the manner due to Neumann, wherein strain gradients at both ends are known and individual strains are not. This approach enables the shear strain distributions of the adhesive joint to be intuitively approximated in a realistic manner without solving the equation. For instance, the strain distributions can be expressed as a continuous function with

opposite signs of the strain gradients at each end of the joint with the characteristic shape as illustrated in Figure 5. It is assumed that the adhesive joint has no disbonded areas that can affect the shear strain distributions.

(5) Equilibrium Eqs. (5) and (6) ignore the bending couples, and the longitudinal stress acting on the adhesive element, as depicted in Figure 4, since the adhesive is assumed to be relatively thin and flexible. In addition, hoop stresses and radial displacements of adherends are also neglected. The introduction of these parameters would result in more complex mathematics and undermine the purpose of a simple approximation method. All $\approx$ signs are used for Eqs. (5) and (6) to indicate that those are only approximated expressions. Later, non-linear FEA is employed for comparison. For scarf angles larger than 10°, all assumptions must carefully be reexamined and other important parameters should also be included; otherwise, strain distributions can be seriously miscalculated. In practice however, to design a strong and efficient joint, a relatively small scarf angle is often selected between 4 and 8°, and typically about 5°, although no rationale for the selections have been explicitly stated in the literature.

(6) Justifications for recently discussed assumptions are based on the nature of axisymmetric responses for the subject scarf configuration wherein the Poisson's ratio-circumferential strains are considered to be

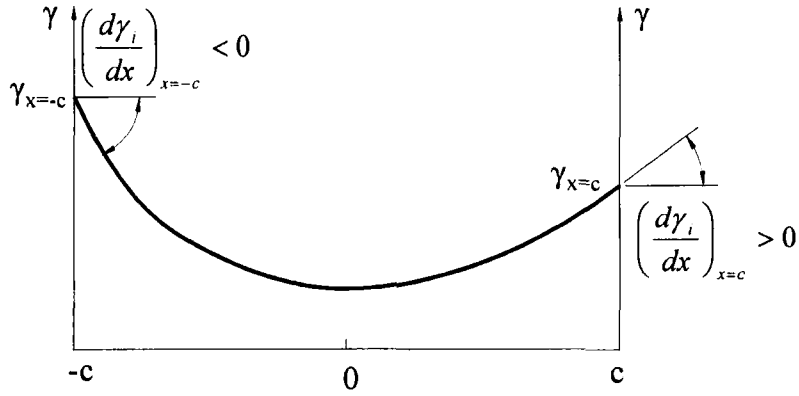

FIGURE 5 γ as a continuous function of x and strain gradients as two boundary conditions.

minutely disrupted through the transition. Confidence in this rationale was reinforced by the correlation between the solutions for plane strain and axisymmetric FEA methods with identical mesh subdivisions for pertinent longitudinal sections pictorially shown in Figure 6.

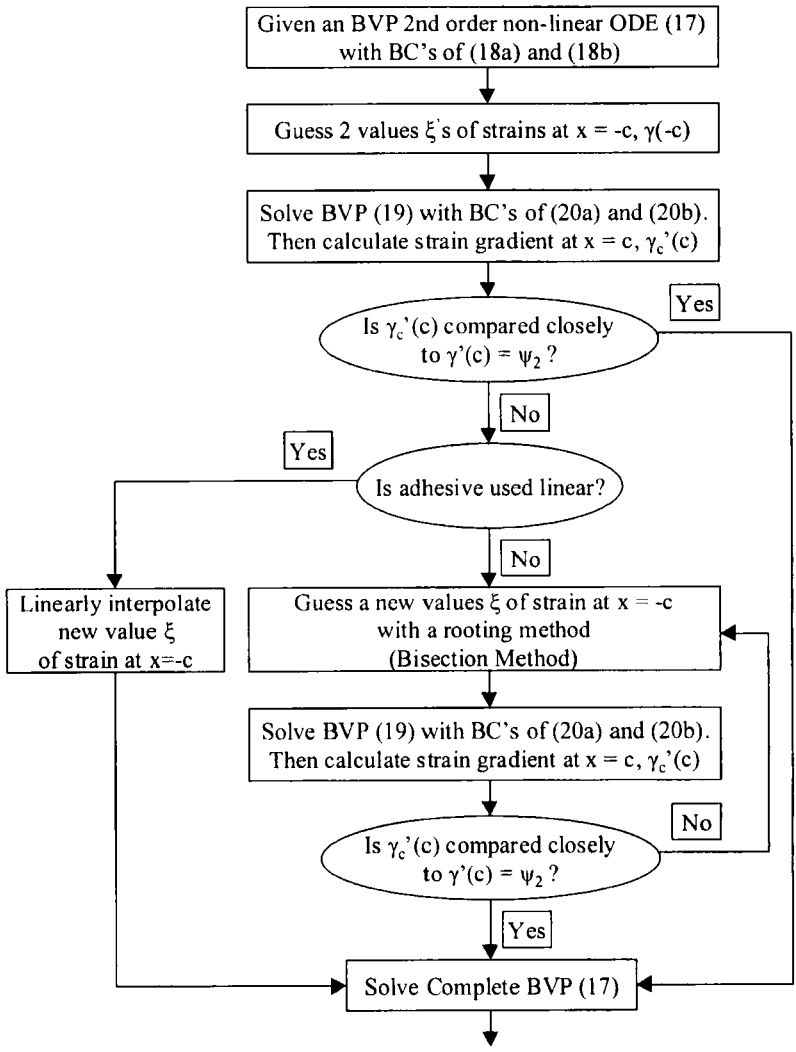

FIGURE 6 Numerical scheme in solving governing Eq. (17) for determination of strain distributions.

However, further scrutiny of these assumptions must be made for cases of widely dissimilar adherends or adherends that possess high degrees of anisotropy.

NUMERICAL METHOD AND FINITE ELEMENT ANALYSIS (FEA)

The derived governing equation is non-linear and contains variable coefficients; thus a solution is more conveniently obtained using a numerical technique. A numerically iterative method based on the Runge-Kutta method is employed since no direct treatment is applicable for this type of equation. A summary of how the proposed method works is presented below.

A general non-linear second-degree boundary value differential equation, such as Eq. (16), is given in the following expression

$$\gamma'' = f(x, \gamma, \gamma') \tag{17}$$

Boundary conditions are given in terms of the derivatives at boundaries as

$$\gamma'(-c) = \psi_1 \tag{18a}$$

$$\gamma'(c) = \psi_2 \tag{18b}$$

The idea here is to guess an appropriate initial value of ξ at $x = -c$, the problem of solving Eq. (17) then becomes solving

$$\gamma'' = f(x, \gamma, \gamma') \tag{19}$$

$$\gamma(-c) = \omega \tag{20a}$$

$$\gamma'(-c) = \psi_1 \tag{20b}$$

The new problem can be easily solved using the standard Runge-Kutta method with a predetermined step size of h. The step size h can be established and optimized by trying a few numbers of

subdivisions to guarantee convergence and avoid solution sensitivity. Then the function value at the opposite end, namely $\gamma_c'(c)$, can be computed. If the result is not suitably close to $\gamma'(c) = \psi_2$ a new ξ is provided. The whole calculation starts over again. Basically, this is an attempt to solve the equation

$$\gamma'(c, \xi) = \psi_2 \tag{21}$$

where ξ considered as an independent variable. Very often, and particularly for the type of non-linear problem found the present study, this equation is non-linear and may be solved by a standard root-finding method, such as Bisection Method, Secant Shooting Method or Newton's Method. When the analysis is limited to essentially linear elasticity of an adhesive, it is then necessary to guess only two values of ξs and the correct ξ can then be linearly interpolated. A detailed summary of the entire numerical scheme is shown in Figure 7.

Finite element software, ANSYS 5.6 [18], is employed to validate the proposed approximation method. All elements are chosen to be eight-node quadrilateral with nominal size dimension equal to one half of the adhesive thickness. The ANSYS Plane 183 axisymmetric element is selected. Figure 6 shows the bonded section of the modeled scarf joint with element distributions. The load is symmetrically distributed to the joint as a uniform pressure applied to all elements at the ends. At all times, the adhesive is assumed to be isotropic. Besides the elastic modulus and the Poisson's ratio, a uniaxial stress–strain characteristic curve is required. The characteristic curve is estimated using the Von Mises equivalent stress concept and shear stress–strain relationship. Consequently, this uniaxial curve is expected to exhibit a representative shear behavior, as the adhesive would be loaded in shear. The "Multi-linear Isotropic Hardening" option of ANSYS is selected for a possible large strain analysis.

The method of solution selected is incremental. The number of sub-steps is set to be from a minimum of 5 to a maximum of 50 with nominal steps of 10. Stress and strain outputs are obtained from all middle nodes of the adhesive layer. Both global x-y stresses and strains, produced by ANSYS 5.6 are converted into shear components for comparison, with calculations from the developed method.

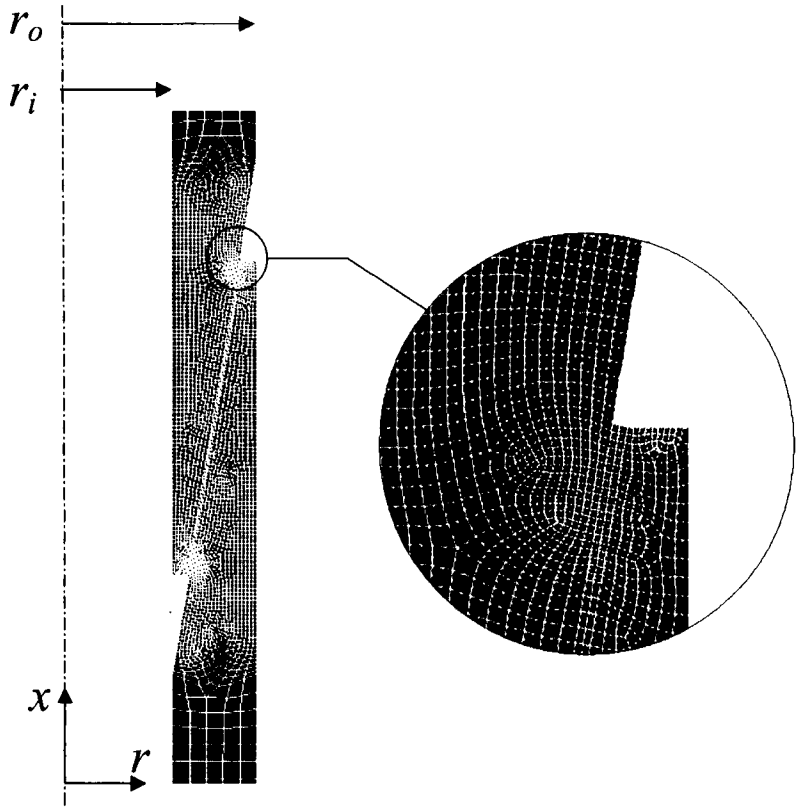

FIGURE 7 Finite element modeling of the bonded section.

The shear strain conversion based on a simple strain transformation is as follows

$$\gamma_a = \gamma_{xy}(\cos^2\alpha - \sin^2\alpha) + 2(\varepsilon_y - \varepsilon_x)\sin\alpha\cos\alpha \qquad (22)$$

NUMERICAL EXAMPLE AND DISCUSSION

Adherends chosen for the numerical analyses are aluminum alloy. Hysol EA9394, a twopart paste adhesive manufactured by Dexter Aerospace [16] is selected for bonding of the adherends. The adhesive

shear properties, which are obtained from the adhesive manufacturer, are generated by a thick adherend shear test with 0.127 mm (0.005 inch) adhesive thickness and aluminum adherends in accordance with ASTM D-5656. Data used for prediction based on both the approximate and FEA methods are as follows

(1) Joint geometry

Outside radius	$r_o = 12.700$ mm (0.500 inch)
Inside radius	$r_i = 9.525$ mm (0.375 inch)
Truncation	$t_c = 0.508$ mm (0.020 inch)
Adhesive thickness	$t_a = 0.127$ mm (0.005 inch)
Scarf angle	$\alpha = 10°$

(2) Aluminum adherends

Elastic modulus	$E_1 = E_2 = 68.946$ GPA (10 Mpsi)
Poisson's ratio	$\nu_1 = \nu_2 = 0.33$

(3) Adhesive

Elastic modulus	$E_a = 4.206$ GPA (0.61 Mpsi)
Shear modulus	$E_a = 1.448$ GPA (0.21 Mpsi)

The non-linear shear stress–strain equation used for the approximate method is obtained by curve-fitting Eq. (1) using experimental data provided by the manufacturer and is plotted in Figure 8

$$\tau = 3.447325\gamma + 51.709875(1 - e^{-36.75\gamma}) \tag{23}$$

The non-linear uniaxial stress–strain relationship used for FEA is derived from the equivalent stress concept as follows

$$\sigma = 10.341975\varepsilon + 89.564130(1 - e^{-63.65\varepsilon}) \tag{24}$$

The detailed derivation is shown in Appendix I.

Various load cases are analyzed, 11.12 KN (2500 lbs), 22.24 KN (5000 lbs) and 33.36 KN (7500 lbs) of direct tensile loads. The total number of steps used for all numerical calculations based on the previously proposed method is selected to be 100. The final solutions are found by making a sufficient number of systematic guesses with an allowable convergence error of less than 1%. Since strain distributions

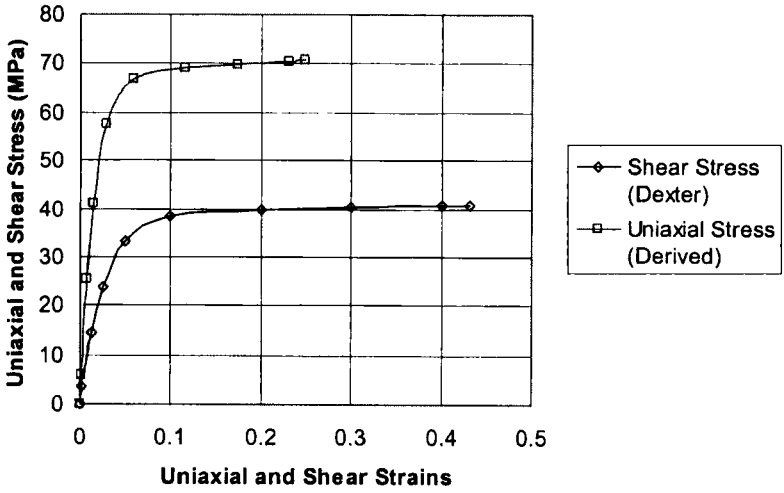

FIGURE 8 Shear and uniaxial stress–strain relationships of EA9394 adhesive.

are continuous and strain values should vary between 0 and the absolute maximum strain, $|\gamma_u|$ for a practical problem, 0 and γ_u are chosen first as two initial guesses. Then subsequent guesses are selectively established using the Bisection Method. Typically, each guess takes approximately from four to seven seconds to complete in MATHCAD 8 software system [19]. Two representative cases studied, *i.e.*, a scarf and a lap joint configuration, both loaded at 22.24 KN (5000 lbs),are displayed in Tables I and II, respectively, where

$\gamma(-c)=\varepsilon$ is guessed strain at $x=-c$
$\gamma'(-c)=\psi_1$ is given strain gradient at $x=-c$
$\gamma'(c)=\psi_2$ is given strain gradient at $x=c$
$\gamma_c'(c)$ is calculated strain gradient at $x=c$, based on guessed $\gamma(-c)$ and given $\gamma'(-c)$

In each table, the rationale of new guesses is clearly identified in the notes column.

Finite Element Analyses are performed for the same number of load cases. Each non-linear analysis for tension requires a relatively extensive time period to reach the final solutions. Due to the fine FEA mesh size selection; only strain values at nodes at 1.27 mm (0.05 inch) increments of the normalized length are plotted for clarity

TABLE I A detailed example of representative strain calculations for a 10°-scarf joint in tension with 22.24 KN (5000 lbs) of axial load

Guess g	$\gamma(-c)$ *guessed*	$\gamma'(-c)$ *given*	$\gamma'_c(c)$ *calculated*	$\gamma'(c)$ *given*	*Notes* (*How a successive guess is made*)
1	0.420000	−0.349	1.744	0.334	$\gamma'_c(c) > \gamma'(c)$, $g_2 < g_1$, $g_2 = g_1/2$
2	0.210000	−0.349	1.675	0.334	$\gamma'_c(c) > \gamma'(c)$, $g_3 < g_2$, $g_3 = g_2/2$
3	0.105000	−0.349	1.578	0.334	$\gamma'_c(c) > \gamma'(c)$, $g_4 < g_3$, $g_4 = g_3/2$
4	0.052500	−0.349	0.836	0.334	$\gamma'_c(c) > \gamma'(c)$, $g_5 < g_4$, $g_5 = g_4/2$
5	0.026250	−0.349	−1.30E152	0.334	$\gamma'_c(c) > \gamma'(c)$, $g_6 > g_5$, $g_6 = (g_5 + g_4)/2$
6	0.039375	−0.349	−1.70E17	0.334	$\gamma'_c(c) < \gamma'(c)$, $g_7 > g_6$, $g_7 = (g_6 + g_4)/2$
7	0.045938	−0.349	−1.022	0.334	$\gamma'_c(c) < \gamma'(c)$, $g_8 > g_7$, $g_8 = (g_7 + g_4)/2$
8	0.049219	−0.349	0.451	0.334	$\gamma'_c(c) > \gamma'(c)$, $g_9 < g_8$, $g_9 = (g_8 + g_7)/2$
9	0.047578	−0.349	0.082	0.334	$\gamma'_c(c) < \gamma'(c)$, $g_{10} < g_9$, $g_{10} = (g_9 + g_8)/2$
10	0.048398	−0.349	0.298	0.334	$\gamma'_c(c) < \gamma'(c)$, $g_{11} > g_{10}$, $g_{11} = (g_{10} + g_8)/2$
11	0.048809	−0.349	0.380	0.334	$\gamma'_c(c) > \gamma'(c)$, $g_{12} < g_{11}$, $g_{12} = (g_{11} + g_{10})/2$
12	0.048604	−0.349	0.341	0.334	$\gamma'_c(c) > \gamma'(c)$, $g_{13} < g_{12}$, $g_{13} = (g_{12} + g_{10})/2$
13	0.048501	−0.349	0.320	0.334	$\gamma'_c(c) < \gamma'(c)$, $g_{14} > g_{13}$, $g_{14} = (g_{13} + g_{12})/2$
14	0.048552	−0.349	0.331	0.334	$\gamma'_c(c) = \gamma'(c)$, solution found

TABLE II A detailed example of representative strain calculations for a lap joint in tension with 22.24 KN (5000 lbs) of axial load

Guess g	$\gamma(-c)$ *guessed*	$\gamma'(-c)$ *given*	$\gamma'_c(c)$ *calculated*	$\gamma'(c)$ *given*	*Notes* (*How a successive guess is made*)
1	0.420000	−0.627	1.205	0.543	$\gamma'_c(c) > \gamma'(c)$, $g_2 < g_1$, $g_2 = g_1/2$
2	0.210000	−0.627	1.17E+00	0.543	$\gamma'_c(c) > \gamma'(c)$, $g_3 < g_2$, $g_3 = g_2/2$
3	0.105000	−0.627	1.009	0.543	$\gamma'_c(c) > \gamma'(c)$, $g_4 < g_3$, $g_4 = g_3/2$
4	0.052500	−0.627	−1.81E+20	0.543	$\gamma'_c(c) < \gamma'(c)$, $g_5 > g_4$, $g_5 = g_4 + g_3)/2$
5	0.078750	−0.627	−8.80E−02	0.543	$\gamma'_c(c) < \gamma'(c)$, $g_6 > g_5$, $g_6 = (g_5 + g_3)/2$
6	0.091875	−0.627	0.858	0.543	$\gamma'_c(c) > \gamma'(c)$, $g_7 < g_6$, $g_7 = (g_6 + g_5)/2$
7	0.085313	−0.627	0.676	0.543	$\gamma'_c(c) > \gamma'(c)$, $g_8 < g_7$, $g_8 = (g_7 + g_5)/2$
8	0.082031	−0.627	0.482	0.543	$\gamma'_c(c) < \gamma'(c)$, $g_9 > g_8$, $g_9 = (g_8 + g_7)/2$
9	0.083672	−0.627	0.596	0.543	$\gamma'_c(c) > \gamma'(c)$, $g_{10} < g_9$, $g_{10} = (g_9 + g_8)/2$
10	0.082852	−0.627	0.545	0.543	$\gamma'_c(c) = \gamma'(c)$, solution found

except in the region of the joint terminations where more strain values are used. The approximate and FEA results in terms of shear stress and strain distributions are plotted in Figures 9, 10 and 11. Normal strain and stress magnitudes are assumed to be relatively small; thus, they are not considered in the comparison.

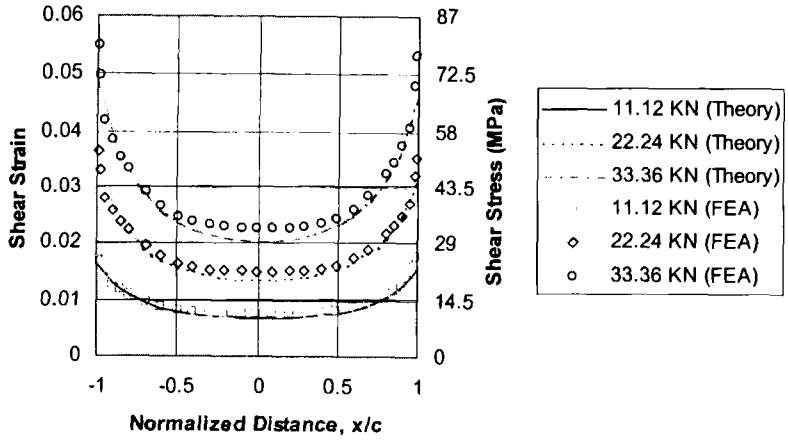

FIGURE 9 Strain and stress distributions of a 10°-scarf joint in tension with linearly elastic representation of adhesive EA9394.

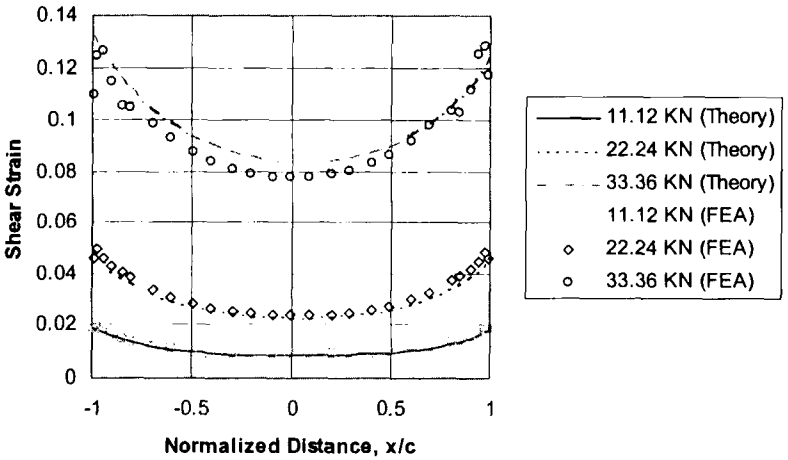

FIGURE 10 Strain distributions of a 10°-scarf joint in tension with proposed non-linear representation of adhesive EA9394.

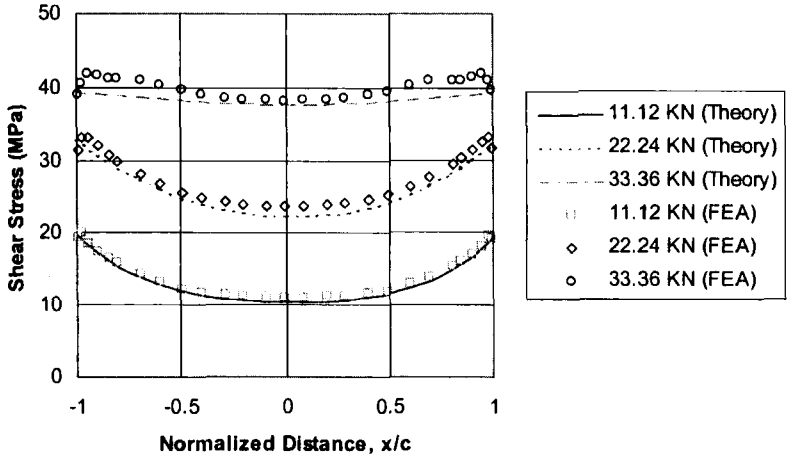

FIGURE 11 Stress distributions of a 10°-scarf joint in tension with proposed non-linear representation of adhesive EA9394.

In general, adhesive shear strain distributions exhibit the same form of the continuous function as predicted earlier. Both the shear stress and the strain distributions look consistent and in good agreement with FEA results. Linear analyses underestimate the shear strains in the central region by about 10%, while in contrast, non-linear analyses overestimate the shear strains by about 8% when compared with the FEA results. Similar observations are also obtained near the joint terminations where the predictions based on linear shear strain analyses underestimate the strain values by 11%. The corresponding predictions based on non-linear shear strain analyses overestimate strain values by 2%. As a consequence, the non-linear analyses of shear strain generally provide more conservative predictions than the linear analyses.

In all approximate solutions, shear strains and stresses do not approach zero at the joint terminations. This is theoretically reconcilable and represents a classical limitation for all predictive methods based on the shear lag theory using differential strain assumptions. However, a tubular joint can be considered geometrically analogous to the double-lap joint in which eccentric bending is not a major concern due to symmetry. In addition, the approximate approach can be found useful for design purposes and for initial failure predictions by simply

neglecting the edge effect, which occurs only on the order of one adhesive thickness from the free edges. Generally, there exist a few disagreements between the developed theory and FEA in the numerical examples but they are typically unsubstantial. Thus, the selected 10°-scarf angle appears to be sufficiently small for the theory to be satisfactorily applicable.

The linear analyses exhibit fairly small shear strains but exceedingly high shear stresses, shown in Figure 9, in comparison with the nonlinear analyses at higher loads, shown in Figures 10 and 11. This is due to the assumption of a linear shear stress–strain relationship that results in overestimation of the adhesive's instantaneous shear modulus at larger strain levels. On the other hand, when the adhesive's behaves nonlinearly, strains increase more rapidly with increasing load especially after passing the transition region where the stress–strain curve makes an abrupt change in slope. The change appears to occur at an absolute shear strain value in the region of 0.08 as seen in Figure 8. In practice, this transition strain value may be considered as an upper limit for a conservative joint design. The entire joint may not have completely failed as the maximum shear strain in the adhesive is reached but additional loading would not generally be recommended. This recommendation is to avoid the potential structural instability resulting in large displacements that may contribute to catastrophic failure. Perhaps, if either the maximum shear stress or the maximum shear strain is established as the failure criterion, the adoption of a non-linear analysis is clearly preferred over a linear analysis as a more reliable approach for highly loaded joints.

It is known that severe imbalance of the stiffness of the adherends can cause the termination at the outside surface to suffer a relatively high shear strain level and fail prematurely while the rest of the joint and the other termination are still under relatively low shear strains. Thus, the full potential strength of the adhesive cannot be fully exploited. However, in these sample problems the joint imbalance is quite small as noted from parameters selected, *i.e.*, $A_1E_1 \approx A_2E_2$. These terms are only inversely proportional to the square of the radius, respectively, when two adherend materials are identical as exemplified in this study. For dissimilar or thicker adherends, it may be critically important to design the joint properly so that the imbalance effect can be minimized, *i.e.*, to adjust truncations at the joint terminations or to

arrange the stiffer adherend inside. It should be acknowledged that the numerical example was intentionally restricted to near-balanced adherends, *i.e.*, adherends with the same modulus and geometry. The objective of the restriction was based on establishing an acceptable approximation, supported not only through correlation with FEA, but also in comparison with experimental work to be presented in a subsequent paper. However, the above theoretical formulation should provide a reasonable approximation for an unbalanced joint involving isotropic adherends with modest differences in modulii and geometry. In future research, further development work that could be applied non-isotropic adherends is also contemplated.

The special case of a scarf joint having $\alpha = 0$ is also investigated. This special case is actually a standard lap joint configuration. The lap joint with a lap length of $2c/\cos(\alpha)$ has the same bonded area as the 10°-scarf joint. Only the results of non-linear analyses based the proposed theory are presented. Shear strain and stress distributions produced by both cases are plotted in Figures 12 and 13 for the same three representative loads as previously exemplified. The 10°-scarf joint seems to be more efficient in terms of lower peak shear strains at the joint terminations and to exhibit more uniform shear strain distributions throughout. The maximum adhesive shear strains of the

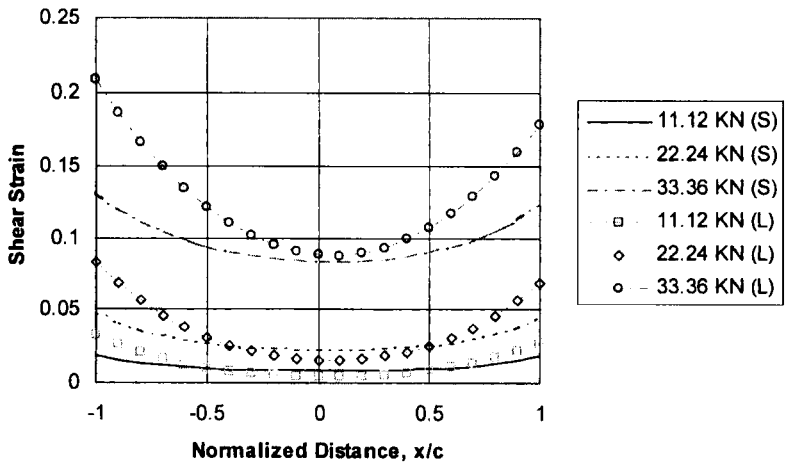

FIGURE 12 Strain distributions of 10°-scarf joint and lap joint in tension with proposed non-linear representation of adhesive EA9394.

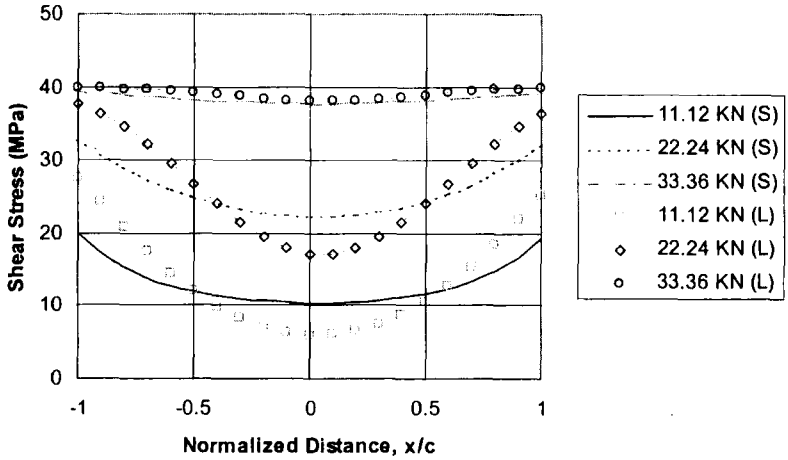

FIGURE 13 Stress distributions of 10°-scarf joint and lap joint in tension with proposed non-linear representation of adhesive EA9394.

lap joint are between 36 and 41% higher in value in the tension load case compared with those of the 10°-scarf joint. The shear strain concentrations of the lap joint, which are defined as the ratio of the strain and the average strain, are correspondingly higher. The shear stress distributions are not obviously distinguishable at the highest load, 33.36 KN (7500 lbs), between 10°-scarf and lap joints although the two strain distributions are significantly different. The observation is the indication of a greater insight to be gained from consideration of shear strain distributions rather than shear stress distributions. From this, it is recognized that the shear strain distributions can offer more guidance in the design and evaluation of predicted joint strength.

Based on this study, a 10° scarf joint may not be the best choice for a design in which creep accumulation, not the maximum load, is a concern [6]. The reason is that in the adhesive the lowest shear stresses of the lap joint are always below the lowest shear stresses of the scarf joint as observed in Figures 12 and 13. The deep elastic troughs found in the shear stress distributions for lap joints can serve as an inhibitor to creep given that the central region remains in an essentially elastic state. In addition, normal stresses in a lap joint, which exist in the vicinities of the joint terminations but quickly dissipate, may result in localized non-catastrophic damage only. In contrast, normal stresses

of a 10° scarf joint certainly exist along the entire lap length, although they are considered to be relatively small in this study. If sufficiently large, the normal stresses can interact with shear stresses to permit extensive propagation of initial damage near terminations. This propagation of damage may then lead to premature failure of the adhesive and an accompanying reduction in joint strength.

CONCLUSION

In this paper, a new approach for calculating non-linear shear strain and stress distributions in the adhesive of a tubular scarf joint subjected to a tension loading condition is proposed. This analytical model represents an extension of the well-established shear-lag theory using differential strain assumptions that were introduced by Volkersen and have been used in numerous adhesive joint researches for many years. There are a few known limitations associated with the non-linear adaptation of this theory; however, it is proposed that such limitations have insignificant effect on failure prediction and on distributions of shear strain and stress for the specific configuration considered.

Another significant contribution of this study is the introduction of a non-linear elastic plastic idealization, which is adopted to model the shear behavior of the selected adhesive. The idealization is basically a combination of linear and exponential functions and is explicitly expressed in terms of stress. Indeed, the stress-explicit form of the adhesive idealization facilitates convenient derivation of the governing equation. The proposed form of adhesive nonlinearity allows the model to obey essentially linear elasticity at low loads and exponential plasticity at high loads, a typical characteristic observed for many adhesives as predominantly loaded in shear.

Both linear and non-linear analyses are conducted. The shear strain and shear stress distributions in the adhesive predicted by the proposed theory have shown to be in acceptably close agreement with the FEA results. The 10°-scarf angle that is selected as the upper limit of analysis capability is found to be sufficiently small to justify application of the proposed theory. Linear analyses exhibit conservative shear stress distributions while showing severely underestimated shear strain distributions in comparison with non-linear analyses which

can be recommended as a more reliable approach for design purposes. The 10°-scarf joint provides higher performance in static load with lower peak shear strains and more uniform shear strain distributions when compared with the lap joint. However, with the deep elastic trough in the middle of the joint and negligible normal stress throughout, the lap joint will typically be a better choice for a sustained loading condition.

NOMENCLATURE

Joint Geometry

α	Scarf angle
t_a	Adhesive thickness
t_c	Truncation thickness
r_o, r_i	Tube outside radius, inside radius
r_m	Tube mean radius
r, θ, x	Cylindrical coordinates
c	Half lap length in case of a truncated joint
A	Bonded area
A_1, A_2	Cross section area at x of adherend 1, adherend 2

Material Properties

E_1, E_2	Elastic modulus of adherend 1, of adherend 2
E_a, G_a	Elastic modulus, shear modulus of adhesive
τ_u	Ultimate shear stress of adhesive
γ_u	Ultimate shear strain of adhesive

Mechanics

N	Total applied tensile load
N_1, N_2	Tensile load on an infinitesimal slice at x on adherend 1, adherend 2
τ_a, σ_a	Shearstress, normal stress in adhesive under tension
γ_a, ε_a	Shear strain, normal strain in adhesive under tension
u_1, u_2	Axial displacement of adherend 1, adherend 2 under tension
ε_1, ε_2	Axial shear strain of adherend 1, adherend 2 under tension

Mathematics and Numerical Analysis

τ, γ	Generic shear stress, shear strain
γ', γ''	Generic strain gradient, rate of change of strain gradient
k	Exponential coefficient of an adhesive model
B_0, B_1	Fitting coefficients of an adhesive model
η, μ	Simplification factors in governing equations
Ψ_1, Ψ_2	Neumann boundary conditions
ξ	Guessed boundary condition
$\gamma_c(-c)$	Calculated strain at $x = -c$

References

[1] Lubkin, J. L., "Theory of adhesive scarf joints", *ASME paper 56-A-52* pp. 255–260 (11-1956).

[2] Adams, R. D. and Peppatt, N. A., "Stress analysis of adhesive bonded tubular lap joints", *Adhesion* **9**, 1–18 (1977).

[3] Chen, D. and Chang, S., "Stress distribution in plane scarf and butt joints", *Trans. ASME* **57**, 78–83 (3-1990).

[4] Thein, W., "Plane stress analysis of a scarf joint", *Internat. J. Solids Structures* **12**, 491–500 (1976).

[5] Hart-Smith, L. J., "Adhesive-bonded scarf and stepped-lap joints", Douglas Aircraft Co., *NASA Langley Research Center Report CR-112237* (1-1973).

[6] Hart-Smith, L. J., "Further Developments in the Design and Analysis of Adhesive-Bonded Structural Joints", *Joining of Composite Materials*, **ASTM STP 749**, 3 (1981).

[7] Volkersen, O., "Die Nietkraftverteilung in zengbeanspruchten Nietverbindungen mit Konstanten Laschenquerschnitten", *Luftfahrtforschung* **15**, 41–47 (1938).

[8] Hart-Smith, L. J., In: *Developments in Adhesives-2*, Kinloch, A. J. Ed. (Applied Science Pub., London, 1981), p. 1.

[9] *ESDU Engineering Sciences Data Unit Report No. 79016*, London, UK (1979) (Inelastic Shear Stresses and Strains in the Adhesives Bonding Lap Joints Loaded in Tension or Shear).

[10] Lee, K. J., Small, J. W. and Miller, V., "The Non-Linear Analysis of Bonded Joints", Hughes Aircraft Company, *19th International SAMPE Technical Conference* pp. 76–86 (10-1987).

[11] Nagaraja, Y. R. and Alwar, R. S., "Non-linear Analysis of an Adhesive Tubular Lap Joint", *J. Adhesion* **10**, 97–106 (1979).

[12] Adams, R. D. and Mallick, V., "The Effect of Temperature on the Strength of Adhesively Bonded Composite Aluminum Joints", *J. Adhesion* **43**, 17–33 (1993).

[13] Eastland, C., Rix, C. and Eisenreich, T., "*Test Strategy and Data Reduction Method for the Thick Adherend Test Procedure*", internal paper General Dynamics/ Space Systems Division, Private Communication, paper received on 2-2000.

[14] Tomblin, J., Pierre, H. and Yang, C., "Adhesive Behavior in Aircraft Application", *Adhesive Joining Technology Review and Workshop*, Santa Barbara, California, USA (11-1999).

[15] Krieger, R. B. Jr., "Stress Analysis Concepts for Adhesive Bonding of Aircraft Primary Structure", Adhesive Bonded Joints: *Testing, Analysis, Design*, **ASTM STP 981**, 264–275 (1988).

[16] *Dexter Hysol EA9394 Specification and Test Data*, Private Communication, papers received on 1-2000.
[17] Adams, R. D., Atkins, R. W., Harris, J. A. and Kinloch, A. J., "Stress Analysis and Failure Properties of Carbon-Fibre-Reinforced-Plastics/Steel Double-Lap Joints", *J. Adhesion* **20**, 29–53 (1986).
[18] ANSYS 5.6 by Swanson Inc.
[19] MathCad by Mathsoft Inc.

APPENDIX I: EQUIVALENT STRESS AND STRAIN DERIVATION

The following derivation will generate a uniaxial stress strain curve from a shear stress strain curve measured in a shear test. This ensures a shear representative behavior to be carried into FEA calculations. In theory, a relationship between pure uniaxial tension (or compression) and pure shear of an isotropic material can be obtained by using the Von Mises equivalent stress concept.

The definition of the equivalent stress based on Von Mises yield criterion is

$$\sigma_{eq} = \sqrt{\frac{3}{2} S_{ij} S_{ij}} \tag{A.1}$$

or

$$\begin{aligned} \sigma_{eq} &= \sqrt{\frac{3}{2}\left(\sigma_{ij} - \frac{1}{3}\sigma_{kk}\delta_{ij}\right)\left(\sigma_{ij} - \frac{1}{3}\sigma_{kk}\delta_{ij}\right)} \\ &= \sqrt{\frac{3}{2}\left(\sigma_{ij}\sigma_{ij} - \frac{1}{3}\sigma_{kk}\right)} \end{aligned} \tag{A.2}$$

When a material is subjected to uniaxial loading, either tension or compression, σ_x is

$$\sigma_{eq} = \sigma_x \tag{A.3}$$

When a material is subjected to pure shear loading, σ_{xy}(or τ_{xy}) is

$$\sigma_{eq} = \sqrt{3}\tau_{xy} \tag{A.4}$$

Comparison of Eqs. (A.3) and (A.4) leads to the expression

$$\sigma_x = \sqrt{3}\tau_{xy} \tag{A.5}$$

The Von Mises criterion may also be expressed in terms of strains as

$$\varepsilon_{eq} = \sqrt{\frac{2}{3}\varepsilon_{ij}\varepsilon_{ij}} \tag{A.6}$$

or

$$\begin{aligned}\varepsilon_{eq} &= \sqrt{\frac{2}{3}\left(\varepsilon_{ij} - \frac{1}{3}\varepsilon_{kk}\delta_{ij}\right)\left(\varepsilon_{ij} - \frac{1}{3}\varepsilon_{kk}\delta_{ij}\right)} \\ &= \sqrt{\frac{3}{2}\left(\varepsilon_{ij}\varepsilon_{ij} - \frac{1}{3}\varepsilon_{kk}\right)}\end{aligned} \tag{A.7}$$

When a material is subjected to uniaxial loading, either tension or compression, ε_x is

$$\varepsilon_{eq} = \varepsilon_x \tag{A.8}$$

When a material is subjected to pure shear loading, ε_{xy} (or $\delta_{xy}/2$)

$$\varepsilon_{eq} = \frac{2}{\sqrt{3}}\varepsilon_{xy} \tag{A.9}$$

Comparison of Eqs. (A.9) and (A.10) leads to the expression

$$\varepsilon_x = \frac{2}{\sqrt{3}}\varepsilon_{xy} = \frac{\gamma_{xy}}{\sqrt{3}} \tag{A.10}$$

By mapping Eqs. (A.5) and (A.10) into Eq. (1), a representative uniaxial stress–strain relationship can be found and utilized for FEA as follows:

$$\sigma = 3B_0\varepsilon + B_1\sqrt{3}\left(1 - e^{-k\varepsilon\sqrt{3}}\right)$$